01 Jan 1974

Magnetic Properties of Cadmium Manganese Ferrite

B. W. Jong

P. D. Ownby
Missouri University of Science and Technology, ownby@mst.edu

Recommended Citation

B. W. Jong and P. D. Ownby, "Magnetic Properties of Cadmium Manganese Ferrite," *IEEE Transactions on Magnetics*, Institute of Electrical and Electronics Engineers (IEEE), Jan 1974.
The definitive version is available at https://doi.org/10.1109/TMAG.1974.1058444

MAGNETIC PROPERTIES OF CADMIUM MANGANESE FERRITE

Bing W. Jong and P. Darrell Ownby

ABSTRACT

The room-temperature saturation magnetization of $Cd_xMn_{1-x}Fe_2O_4$ decreased with increasing cadmium concentration. When $0 < x \leqslant 0.5$, the decrease in saturation magnetization was due to the increase in the amount of non-magnetic distorted cubic $Cd(Mn,Fe)_2O_4$ which formed as x was increased. The saturation magnetization became very small for $x > 0.5$ due to the formation of $(Cd,Fe)(Mn,Fe)_2O_4$.

The grain size, the grain size distribution and the porosity played a significant role in changing the hysteresis loop parameters of $Cd_xMn_{1-x}Fe_2O_4$. The maximum Br/Bm was obtained at x = 0.3 due to the combination of a smaller grain size and a more homogeneous grain size distribution. A higher porosity at x = 0 and a smaller grain size at x = 0.3 accounted for a larger coercive field strength for these compositions.

INTRODUCTION

Eichbaum studied CdMn-ferrites for use in high speed computer components [1]. Eichbaum also studied the effect of boron on square-loop CdMn-ferrites [2]. Cadmium-containing ZnMn-ferrite systems were investigated by Baird et. al. [3]. However, these investigations were not primarily designed to determine the effect of cadmium on the magnetic properties. Moreover, the compositions which they studied were different from those in the present work.

The solid-state reaction sequence and optimum time-temperature and fabrication regime for producing cadmium manganese ferrite have recently been discussed elsewhere [4]. Figure 1 shows the variation in (311) d-spacing of $CdFe_2O_4$ with cadmium concentration, x, when $CdMn_2O_4$ dissolved in $CdFe_2O_4$ for the composition $xCdO + (1-x)MnCO_3 + \alpha\text{-}Fe_2O_3$ reacted at 900°C for 2 hours. The knee in the d-spacing vs. composition curve at x = 0.5 has been described in detail indicating that all of the Mn_3O_4 was dissolved in the $Cd(Mn,Fe)_2O_4$ for $0.5 < x < 1.0$ at this temperature [4]. A single phase of $Cd_xMn_{1-x}Fe_2O_4$ existed at 1150°C. This paper will correlate these results with the magnetic properties.

In this work, the effects of cadmium content on the physical properties, magnetic properties and microstructure were studied. Careful control over processing variables was exercised so that the amount of powder, ball milling parameters, calcination and sintering time-temperature cycles were fixed for each composition batch.

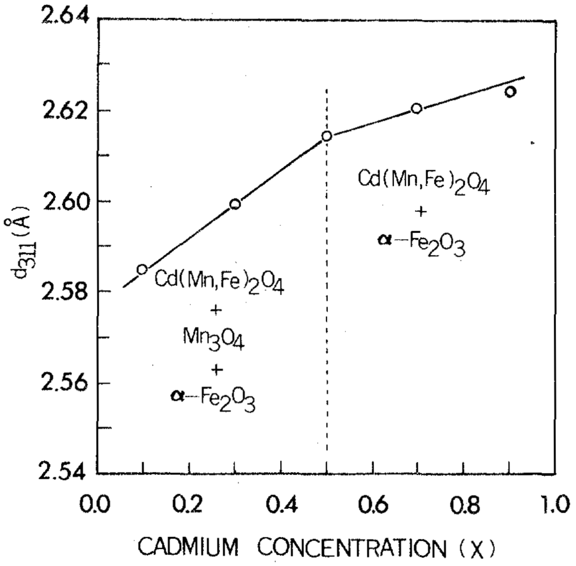

Figure 1. Variation in (311) d-spacing of $CdFe_2O_4$ with cadmium concentration, x, when $CdMn_2O_4$ dissolved in $CdFe_2O_4$ for the composition $xCdO + (1-x)MnCO + \alpha\text{-}Fe_2O_3$ reacted at 900°C for 2 hours.

EXPERIMENTAL

A. Sample Preparation

100-gram batches with composition $xCdO+(1-x)MnCO_3 + \alpha\text{-}Fe_2O_3$, where x = 0.0, 0.1, 0.2, 0.3, 0.4, 0.5, 0.6, 0.7 and 0.9 were calcined at 900°C for 2 hours. The percent of $Cd(Mn,Fe)_2O_4$ formed was calculated from X-ray diffraction intensities as follows:

$$\text{Percent conversion} = I_{311}[Cd(Mn,Fe)_2O_4] \times 100/\{I_{311}[Cd(Mn,Fe)_2O_4] + I_{111}(CdO) + I_{211}(Mn_3O_4) + I_{104}(\alpha\text{-}Fe_2O_3)\}$$

Distilled water slurries containing 60% solids were steel-ball milled for 16 hours. The dried and granulated calcined powder was uniaxially pressed at 4.22×10^5 kg/m^2 into 1.91 cm diameter, 0.32 cm high pellets and into 3.66 cm outside diameter, 2.77 cm inside diameter, by 0.51 cm high toroids and then isostatically pressed to 1.76×10^7 kg/m^2.

The pellets and toroids were sintered side-by-side, in air, in tightly covered cylindrical alumina crucibles at 1150°C for 30 minutes and air-quenched. The sintered pellets were then used for the measurements of sintered density, saturation magnetization and characterization of microstructure. The sintered toroids were used for studies of hysteresis-loop parameters.

B. Measurement

X-ray densities were calculated from unit cell dimensions obtained by standard X-ray technique. Sintered densities were measured by using Archimedes' principle.

Saturation magnetization was measured at room temperature using a vibrating sample magnetometer and an applied field of 5 kOe. The standard against which the CdMn-ferrite spheres were compared was a 99.999% nickel which was checked by various laboratories in the ferrite industry. The 4πMs of Ni was 6100 G.

Manuscript received March 25, 1974; revised May 22, 1974. Paper 9.9, presented at the 1974 INTERMAG conference Toronto, Canada, May 14-17. This work was supported by a fellowship grant from the Emerson Electric Co.

B. W. Jong was with the Department of Ceramic Engineering, University of Missouri-Rolla, Rolla, Mo. 65401. He is now with Engineering Experiment Station, Georgia Institute of Technology, Atlanta, Georgia 30332.

P. D. Ownby is with the Department of Ceramic Engineering and Graduate Center for Materials Research, University of Missouri-Rolla, Rolla, Mo. 65401.

The measurements of Br/Bm and coercive field strength were made using an a-c dynamic method described by Soohoo [5]. Br/Bm is defined as the ratio of the remanent magnetization, Br, to the maximum magnetization, Bm, at a drive of 5 Oe.

Microstructures were characterized using a scanning electron microscope.

RESULTS AND DISCUSSION

A. Relative Density

The theoretical and sintered density as a function of cadmium concentration are plotted in Figure 2. It can be seen that all cadmium concentrations studied increased the relative density to ∿98% of theoretical whereas without cadmium, only ∿89% of the theoretical value was reached.

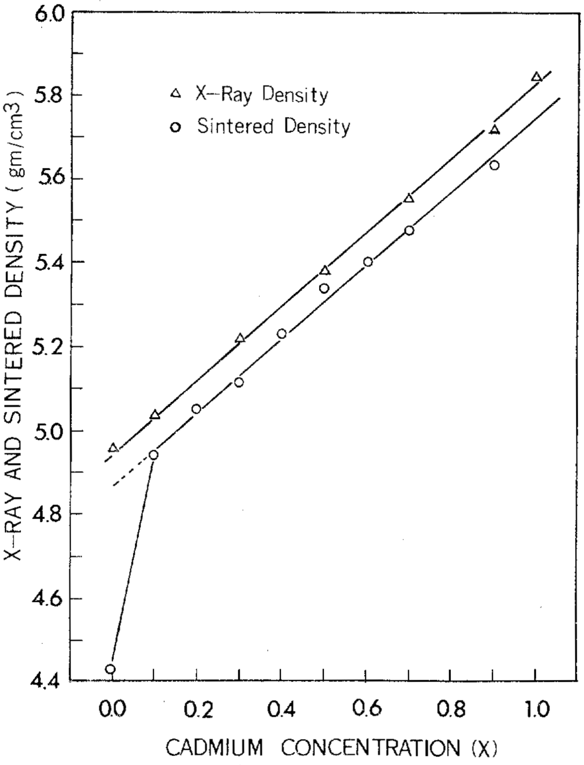

Figure 2. X-ray density and sintered density vs. cadmium concentration, x, for $Cd_xMn_{1-x}Fe_2O_4$. Specimens were sintered at 1150°C for 30 minutes.

B. Magnetic Properties

As far as the authors have been able to determine this is the first and most complete characterization of cadmium manganese ferrite published to date. The changes in the saturation magnetization, Br/Bm and coercive field strength were measured as the cadmium concentration, x, was increased.

a. Saturation magnetization

Figure 3 shows the measured room-temperature saturation magnetization, $4\pi Ms$, versus Cd concentration, x, in the solid solution of $Cd_xMn_{1-x}Fe_2O_4$ and percent conversion to $Cd(Mn,Fe)_2O_4$ versus Cd concentration, x, for the composition $xCdO + (1-x)MnCO_3 + \alpha\text{-}Fe_2O_3$ reacted at 900°C for 2 hours. It can be seen that the saturation magnetization of $Cd_xMn_{1-x}Fe_2O_4$ decreased as the non-magnetic phase of $Cd(Mn,Fe)_2O_4$ progressively increased.

The saturation magnetization decreased slowly, as x increased from 0 to 0.2, and then more rapidly to x = 0.5. The percent of $Cd(Mn,Fe)_2O_4$ increased to ∿82% when the Cd concentration, x, was 0.2.

The influence of the cation distribution on the $4\pi Ms$ can easily be understood by considering the solid state formation sequence [4]. The reaction sequence is simplified as follows:

$$\begin{matrix}Fe_2O_3\\Mn_2O_3\end{matrix}\xrightarrow[600^\circ-800^\circ C]{CdO}\begin{matrix}CdFe_2O_4\\CdMn_2O_4\end{matrix}\xrightarrow[900^\circ C]{\qquad}Cd(Mn,Fe)_2O_4$$

$$\xrightarrow[1150^\circ C]{MnFe_2O_4}(Cd,Mn,Fe)(Mn,Fe)_2O_4$$

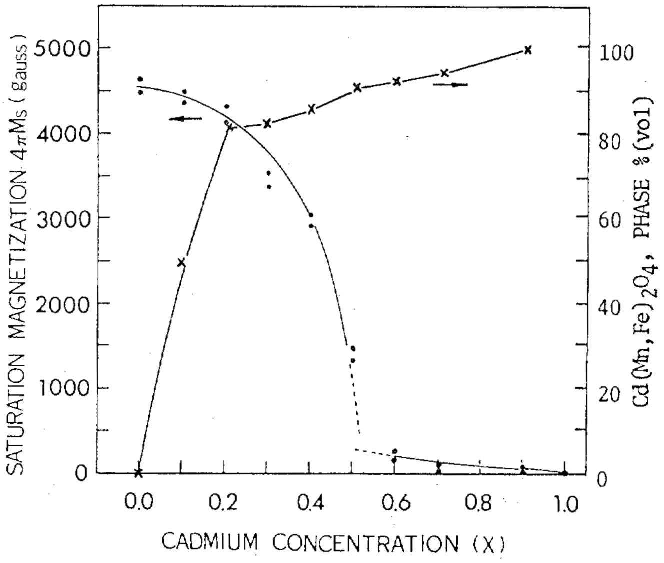

Figure 3. Room-temperature saturation magnetization vs. cadmium concentration, x, for $Cd_xMn_{1-x}Fe_2O_4$ and percent conversion to $Cd(Mn,Fe)_2O_4$ vs. cadmium concentration, x, for the composition $xCdO + (1-x)MnCO_3 + \alpha\text{-}Fe_2O_3$ reacted at 900°C for 2 hours.

At 900°C, all available Cd^{2+} and some Mn^{3+} and some Fe^{3+} have formed $Cd(Mn,Fe)_2O_4$ which coexist with Mn_3O_4 and $\alpha\text{-}Fe_2O_3$. A single phase of CdMn-ferrite formed by the dissolution of $Cd(Mn,Fe)_2O_4$ into $MnFe_2O_4$ at 1150°C. It is known that Cd^{2+} preferentially occupies the tetrahedral sites. When $CdFe_2O_4$, $CdMn_2O_4$ and $Cd(Mn,Fe)_2O_4$ are formed some Mn^{3+} and Fe^{3+} are forced into the octahedral sites. Mn^{3+} is a Jahn-Teller ion [6,7] which will distort the spinel structure. The $Cd(Mn,Fe)_2O_4$ was found to be elongated in the c-axis with $c/a > 1.0$ in all compositions $0 < x < 1.0$ [4]. Baltzer etc. have shown that symmetry distortion can strongly influence the magnetic properties [8]. Jacobs found triangular moment arrangements in the distorted spinel structure $M{\cdot}Mn_2O_4$ [9] in agreement with the Yafet-Kittel model for antiferromagnetic arrangements in ferrite [10]. It appears that the non-magnetic, distorted $Cd(Mn,Fe)_2O_4$ has affected the saturation magnetization of $Cd_xMn_{1-x}Fe_2O_4$. In this composition range, the system can be considered as ∿(0-90%)$Cd(Mn,Fe)_2O_4$ + ∿(100-10%)$MnFe_2O_4$. Obviously, the saturation magnetization of $Cd_xMn_{1-x}Fe_2O_4$ is decreased by increasing the amount of $Cd(Mn,Fe)_2O_4$ dissolving into the $MnFe_2O_4$.

When x = 0.5, the saturation magnetization drops to a very low value and as $x \to 1.0$ it approaches zero. The drop in magnetization was also confirmed by the dynamic hysteresigrams of $Cd_xMn_{1-x}Fe_2O_4$ as shown in Figure 4. No hysteresis loop could be displayed when $x \geqslant 0.6$.

The cation distribution can also be shown from the reaction sequence [4] as follows;

$$\begin{matrix}\mathrm{Fe_2O_3}\\ \mathrm{Mn_2O_3}\end{matrix} \xrightarrow[600^\circ\text{-}800^\circ C]{\mathrm{CdO}} \begin{matrix}\mathrm{CdFe_2O_4}\\ \mathrm{CdMn_2O_4}\end{matrix} \xrightarrow[900^\circ C]{} \mathrm{Cd(Mn,Fe)_2O_4}$$

$$\xrightarrow[1150^\circ C]{\alpha\text{-}\mathrm{Fe_2O_3}} \mathrm{(Cd,Fe)(Mn,Fe)_2O_4}$$

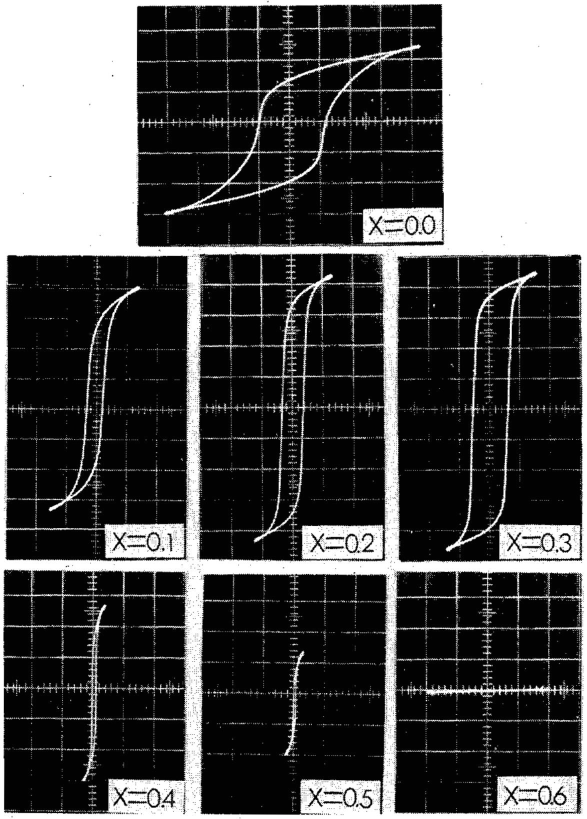

Figure 4. Dynamic 1 kHz hysteresigrams vs. cadmium concentration, x, for $Cd_xMn_{1-x}Fe_2O_4$. Major divisions of vertical scale 600 G; major divisions of horizontal scale 3 Oe.

At 900°C, all available Cd^{2+} and Mn^{3+}, and some Fe^{3+} have formed the $Cd(Mn,Fe)_2O_4$ existing with α-Fe_2O_3. A single phase of $(Cd,Fe)(Mn,Fe)_2O_4$ was formed at 1150°C. In this composition range, the system is $\sim$(90-100%)$Cd(Mn,Fe)_2O_4$ + $\sim$(10-0%)α-Fe_2O_3. The iron appears to be distributed in the tetrahedral and octahedral sites so as to form a solid solution $(Cd,Fe)(Mn,Fe)_2O_4$ which exhibits very low magnetization. The thermal effect on the spin alignment is not considered in this paper. Future work will include a saturation magnetization study of $Cd_xMn_{1-x}Fe_2O_4$ near 0° K and classification of magnetic characteristics of $Cd(Mn,Fe)_2O_4$ and $(Cd,Fe)(Mn,Fe)_2O_4$.

Both Cd and Zn strongly prefer the tetrahedral sites and are non-magnetic. Therefore, a comparison was made for room-temperature $4\pi Ms$ of $Cd_xMn_{1-x}Fe_2O_4$ with the corresponding $Zn_xMn_{1-x}Fe_2O_4$ [11,12,13]. For comparison, the $4\pi Ms$ was corrected to the value which was equivalent to the X-ray density. There are no differences in $4\pi Ms$ for $x = 0$ and $x \geqslant 0.8$. $MnFe_2O_4$ is the same in each case for $x = 0$ and when $x \geqslant 0.8$ for $Zn_xMn_{1-x}Fe_2O_4$ it appears to be similar to when $x > 0.5$ for $Cd_xMn_{1-x}Fe_2O_4$ described previously.

There are substantial differences in the $4\pi Ms$ for $0.2 \leqslant x < 0.8$. $Cd_xMn_{1-x}Fe_2O_4$ has a lower value of $4\pi Ms$ than the corresponding $Zn_xMn_{1-x}Fe_2O_4$ in these compositions. This is probably due to a different ionic radius, (Cd^{2+} is 0.92 Å which is larger than Zn^{2+}, 0.69 Å [14]) resulting in a more distorted spinel, ($CdMn_2O_4$ with $c/a = 1.20$ and $ZnMn_2O_4$ with $c/a = 1.14$ [15,16]).

b. Hysteresis loop parameters

Figure 5 shows the Br/Bm ratio and coercive field strength, at a drive of 5 Oe and 1 kHz, versus cadmium concentration. The coercive field strength of zero cadmium concentration is larger than when $x > 0$ because of the lowered sintered density at $x = 0$. This agrees with Wijn etc. who found that porosity strongly influenced the coercive field strength, pores being non-magnetic inclusions [17]. After the initial drop, as the cadmium concentration increases, both the Br/Bm and the coercive field strength increase reaching a maximum at $x = 0.3$.

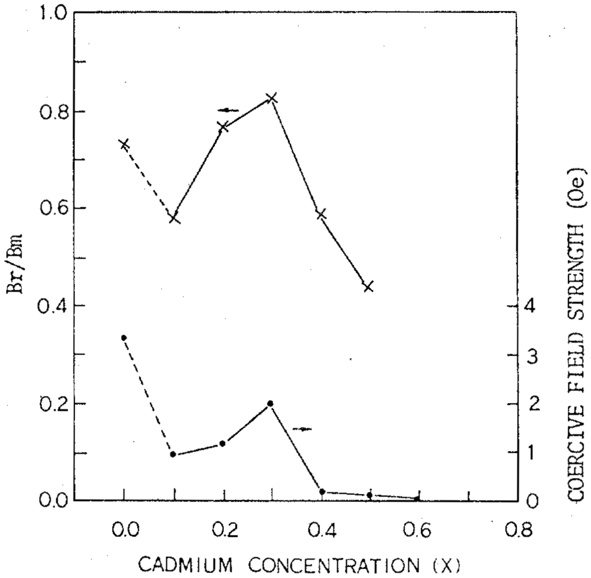

Figure 5. Br/Bm and coercive field strength at a drive of 5 Oe and 1 kHz vs. cadmium concentration, x, for $Cd_xMn_{1-x}Fe_2O_4$.

Microstructures of various composition were characterized using a scanning electron microscope. Beyond $x = 0.3$, the grain size was larger and less homogeneous. The hysteresis loop is microstructure sensitive and also dependent on the intrinsic magnetostriction constant. The present work only considers the microstructure. The grain size and grain size distribution affect the Br/Bm ratio for the solid solution of $Cd_xMn_{1-x}Fe_2O_4$. A smaller grain size and a more homogeneous grain size distribution produce a higher Br/Bm, and a smaller grain size or a higher porosity produce a larger coercive field strength. The microstructure appears to be composition sensitive. A future paper will be written on the magnetostriction and thermodynamic studies of $Cd_xMn_{1-x}Fe_2O_4$.

CONCLUSIONS

It has been shown that the room-temperature saturation magnetization of $Cd_xMn_{1-x}Fe_2O_4$ decreased with increasing cadmium concentration. The fact that the saturation magnetization was correlated to the formation sequence was verified. When $0 < x \leq 0.5$, all available Cd^{2+} preferentially occupy the tetrahedral sites forcing some Mn^{3+} and some Fe^{3+} into the octahedral sites, forming the non-magnetic distorted cubic $Cd(Mn,Fe)_2O_4$ which coexisted with phases of Mn_3O_4 and α-Fe_2O_3 at 900°C. At 1150°C, a single phase of CdMn-ferrite was formed by dissolving $Cd(Mn,Fe)_2O_4$ into $MnFe_2O_4$. The saturation magnetization of CdMn-ferrite was then decreased due to the increase in the amount of $Cd(Mn,Fe)_2O_4$ formation as x was increased. When $0.5 < x < 1.0$, all available Cd^{2+} and Mn^{3+}, and Fe^{3+} formed the $Cd(Mn,Fe)_2O_3$ existing with α-Fe_2O_3 at 900°C. At 1150°C, a single phase of $(Cd,Fe)(Mn,Fe)_2O_4$ was formed, which exhibited very low magnetization.

It has also been shown that the grain size and grain size distribution changed with the Br/Bm ratio and that the porosity or the grain size changed with the value of coercive field strength for $Cd_xMn_{1-x}Fe_2O_4$ and a correlation was inferred.

REFERENCES

[1] B. R. Eichbaum, "Evaluation of New High-Speed Magnetic Ferrite System for Use in Computer Components," J. Appl. Phys., Supplement to vol. 30, pp. 49-52s, April 1959.

[2] B. R. Eichbaum, "Effect of Boron on Square-Loop Cadmium Manganese Ferrites," J. Am. Cer. Soc., vol. 44, pp. 51-54, February 1961.

[3] D. H. Baird, et. al., "Cadmium-Substituted Ferrite Materials," U.S. Patent no. 3,400,169, April 22, 1969.

[4] B. W. Jong and P. D. Ownby, "Formation and Densification of Cadmium Manganese Ferrite," Am. Cer. Soc. Bull., vol. 52, pp. 526-528, June 1973.

[5] Ronald F. Soohoo, "Theory and Application of Ferrites," Prentice-Hall, Inc., Englewood Cliffs, New Jersey, 1960. pp. 110-111.

[6] G. Blasse, "Properties of Magnetic Compounds in Connection with Their Crystal Chemistry," Progress in Ceramic Science, ed. by J. E. Burke, Pergamon Press, vol. 4, pp. 133-193, 1966.

[7] H. A. Jahn and E. Teller, "Stability of Polyatomic Molecules in Degenerate Electronic States I-Orbital Degeneracy," Proc. Roy. Soc. A161, pp. 220-235, 1937.

[8] Philip K. Baltzer and Peter J. Wojtowicz, "On the Origin of Low Moments in Chromium-Containing Spinels," J. Appl. Phys., Supplement to vol. 30, pp. 27s-29s. April 1959.

[9] I. S. Jacobs, "Evidence for Triangular Moment Arrangements in $M \cdot Mn_2O_4$," J. Phys. Chem. Solids, vol. 11, pp. 1-11, 1959.

[10] Y. Yafet and C. Kittel, "Antiferromagnetic Arrangements in Ferrite," Phys. rev. vol. 87, no. 2, pp. 290-294, 1952.

[11] C. Guillaud and H. Vreveaux, "Propriétés Ferromagnétiques des Ferrites Mixtes de Cobalt et de Zinc et de Manganese et de Zinc," C. R. Acad. Sci., vol. 230, pp. 1458, 1950.

[12] E. W. Gorter, "Some Properties of Ferrites in Connection with Their Chemistry," Proceedings of the IRE, vol. 43, pp. 1945-1973, 1955.

[13] Wilhelm H. Von Aulock, "Handbook of Microwave Ferrite Materials," Academic Press, New York, pp. 341-343 and pp. 308, 1965.

[14] F. A. Cotton and G. Wilkinson, "Advanced Inorganic Chemistry," A Comprehensive Text, Interscience Publishers, New York, pp. 45, 1962.

[15] A. P. B. Sinha, N. R. Sanjana and A. B. Biswas, "The Structure of Some Manganites," Acta Cryst. vol. 10, pp. 439-440. 1957.

[16] J. D. Dunitz and L. E. Orgel, "Electronic Properties of Transition-Metal Oxide-I," Distortion from Cubic Symmetry," J. Phys. Chem. Solids, vol. 3, pp. 20-29, 1957.

[17] H. P. J. Wijn, E. W. Gorter, C. J. Esveldt and P. Geldermans, "Conditions for Square Hysteresis Loops in Ferrites," Phillips Technical Review vol. 16, pp. 49-58, 1954.